Optical dispersion relations for amorphous semiconductors and amorphous dielectrics

A. R. Forouhi

IBM Almaden Research Center, 650 Harry Road, San Jose, California 95120-6099

I. Bloomer

Department of Physics, San Jose State University, San Jose, California 95192-0106

An expression for the imaginary part, k, of the complex index of refraction, $N = n - ik$, for amorphous materials is derived as a function of photon energy E: $k(E) = A(E - E_g)^2/(E^2 - BE + C)$ where A, B, and C are positive nonzero constants characteristic of the medium such that $4C - B^2 > 0$. E_g represents the optical energy band gap. The real part, n, of the complex index of refraction is then determined to be $n(E) = n(\infty) + (B_0E + C_0)/(E^2 - BE + C)$ using Kramers-Kronig analysis, where B_0 and C_0 are constants that depend on A, B, C, and E_g, and $n(\infty)$ is a constant greater than unity. Excellent agreement was found between these formulas and experimentally measured and published values of n and k of amorphous silicon, hydrogenated amorphous silicon, amorphous silicon nitride, and titanium dioxide.

I. INTRODUCTION

The complex index of refraction, $N(E) = n(E) - ik(E)$, for amorphous semiconductors and amorphous dielectrics has previously been formulated for a narrow range of energies.[1-9] Nine parameters (as discussed below) must be identified in order to simultaneously describe $n(E)$, the refractive index, and $k(E)$, the extinction coefficient. This narrow range does not include the experimentally observed maxima of $n(E)$ and $k(E)$. Furthermore, the fundamental connection between $n(E)$ and $k(E)$ derived by Kramers and Kronig[10] cannot be applied to this formulation.

Two decades ago, Tauc et al.[1] derived the equation

$$\omega^2\epsilon_2 \propto (\hbar\omega - E_g)^2 \qquad (1)$$

to describe the absorption edge of amorphous semiconductors. $\hbar\omega$ denotes photon energy, E_g the optical energy band gap, and ϵ_2 the imaginary part of the complex dielectric constant $\epsilon = \epsilon_1 - i\epsilon_2$. N is related to ϵ by $\epsilon = N^2$.

It is usually argued that the absorption coefficient, $\alpha = 2\omega k/c$ (and therefore k), can be broken into two parts.[3-6] For $\alpha > \alpha_c$, different variations of Eq. (1) have been used to describe the absorption edge of amorphous semiconductors and dielectrics:[2-6]

$$\epsilon_2 \propto \frac{(\hbar\omega - E_g)^m}{(\hbar\omega)^2}, \text{ with } m = 2 \text{ or } 3; \qquad (2)$$

or

$$k = A_1\frac{(\hbar\omega - E_g)^m}{(\hbar\omega)^2} , \qquad (3)$$

assuming n is effectively constant, since $\epsilon_2 = 2nk$. For $\alpha < \alpha_c$,

$$k = A_2\exp[(\hbar\omega - E_0)/\Gamma]/\hbar\omega . \qquad (4)$$

E_0 is a constant comparable to E_g and Γ is the temperature-dependent width of the exponential tail. The constant A_2 can be determined if the cross-over value of the absorption coefficient, i.e., α_c (numerically in the approximate range of $10^3 - 10^5$ cm^{-1}, depending on the material) is given. The empirical formula (4) is referred to as Urbach's tail.[4]

Theoretically n and k are related by Kramers-Kronig analysis.[10] Spectral dependence of the refractive index n, however, cannot be derived from the above equations for k. Nevertheless, the most commonly used spectral dependence of n, referred to as the Sellmeier equation, (independent of k) is[6-9]

$$n^2(\lambda) = c_1 + \frac{c_2\lambda^2}{\lambda^2 - \lambda_0^2} , \qquad (5)$$

where c_1, c_2, and λ_0 are constants chosen to match experimental data. Equation (5) holds only for wavelengths far from λ_0.

Therefore, according to the previous treatments, nine parameters (α_c, m, A_1, E_g, E_0, Γ, c_1, c_2, and λ_0) are needed to simultaneously specify n and k in a narrow range of energies.

In this paper we derive dispersion relations for $n(E)$ and $k(E)$ which depend on only five parameters. These expressions, which include the observed maxima of $n(E)$ and $k(E)$, closely fit the published data for a wide class of amorphous materials. Moreover, these relations are consistent with Kramers-Kronig analysis.

II. THEORY

We begin by looking at the probability for a transition per unit time, $W_{d\Omega}$ (due to photons contained within the solid angle $d\Omega$) between two arbitrary states, $|a\rangle$ and $|b\rangle$, where $E_b > E_a$. From first-order time-dependent perturbation theory,[11,12]

$$W_{d\Omega} = \frac{\pi e^2}{m_e}\frac{n_{\omega,\alpha}}{\omega}|\langle b|\mathbf{P}\cdot\boldsymbol{\epsilon}^{(\alpha)}|a\rangle|^2\rho_{\omega,d\Omega} . \qquad (6)$$

e, m_e, and $\mathbf{P}$ are the electron charge, mass, and momentum. $n_{\omega,\alpha}$ represents the occupation number for photons

with angular frequency ω and polarization vector $\varepsilon^{(\alpha)}$ ($\alpha = 1,2$ corresponding to two possible polarization states). $\rho_{\omega,d\Omega}\,d\omega$ gives the number of allowed photon states in the frequency range ω to $\omega + d\omega$.

$$\rho_{\omega,d\Omega}\,d\omega = \frac{\kappa^2 d\kappa\,d\Omega}{(2\pi)^3} = \frac{\omega^2\,d\Omega}{(2\pi c)^3}d\omega \ . \tag{7}$$

Equation (6) holds only if $E_b - E_a = \hbar\omega$. The momentum matrix element in (6) can be replaced by the position matrix element since $\langle b \mid \mathbf{P} \mid a \rangle = im_e\omega\langle b \mid \mathbf{x} \mid a \rangle$.[11] Furthermore, the incident intensity, $I_0(\omega)$, can be substituted in Eq. (6) since

$$I_0(\omega)d\omega = n_{\omega,\alpha}c\hbar\omega\rho_{\omega,d\Omega}\,d\omega = \frac{\hbar\omega^3 n_{\omega,\alpha}\,d\Omega}{8\pi^3 c^2}d\omega \ . \tag{8}$$

In terms of these parameters, the transition probability rate W is

$$W = \frac{8\pi^2}{3}\frac{e^2 I_0}{\hbar^2 c}\mid \langle b \mid \mathbf{x} \mid a \rangle \mid^2 \ , \tag{9}$$

where the two independent directions of polarization, $\varepsilon^{(1)}$ and $\varepsilon^{(2)}$, have been summed over and an integration over all propagation directions, $d\Omega$, has been performed.

As pointed out by Heitler,[12] the energy absorbed per unit time, $S(\omega)$, is obtained by multiplying (9) by $\hbar\omega$:

$$S(\omega) = \frac{8\pi^2}{3\hbar c}e^2\omega I_0\mid \langle b \mid \mathbf{x} \mid a \rangle \mid^2 \ . \tag{10}$$

Equation (10) holds only if the excited state $\mid b \rangle$ has an infinite lifetime. [Equation (1) due to Tauc et al.[1] is based on an infinite lifetime.]

If the excited state $\mid b \rangle$ has a finite lifetime, τ, according to first-order time-dependent perturbation theory,[11,12] the absorption probability contains a damping factor:

$$\frac{\hbar^2\gamma}{2\pi}\frac{1}{(E_b - E_a - \hbar\omega)^2 + \hbar^2\gamma^2/4} \ , \tag{11}$$

where $\gamma = 1/\tau$. Then, the energy absorbed in the frequency range ω to $\omega + d\omega$ per unit time, $\Phi(\omega)d\omega$, contains this factor:[12]

$$\Phi(\omega)d\omega = S\frac{\hbar^2\gamma}{2\pi}\frac{1}{(E_b - E_a - \hbar\omega)^2 + \hbar^2\gamma^2/4}d\omega \ . \tag{12}$$

Note, in the limit $\gamma \to 0$,

$$\frac{\hbar^2\gamma}{2\pi}\frac{1}{(E_b - E_a - \hbar\omega)^2 + \hbar^2\gamma^2/4} \to \delta(E_b - E_a - \hbar\omega)$$

so that

$$\lim_{\gamma \to 0}\int \Phi(\omega)d(\hbar\omega) = S(\omega)$$

where $\omega = (E_b - E_a)/\hbar$.

The absorption coefficient $\alpha(\omega)$ is then defined by[12]

$$\alpha(\omega) = \lim_{\Delta x \to 0}\left[-\frac{1}{I}\frac{\Delta I}{\Delta x}\right] = \frac{1}{I_0}\Theta\Phi \ , \tag{13}$$

where Θ represents the number of possible transitions per unit volume in a layer of thickness Δx. Since the extinction coefficient, k, is directly related to $\alpha(\omega)$ by

$$k = \frac{\alpha c}{2\omega} \ , \tag{14}$$

from Eqs. (12), (13), and (14), k is then determined to be

$$k = \Theta\frac{2\pi}{3}e^2\hbar\mid \langle b \mid \mathbf{x} \mid a \rangle \mid^2\frac{\gamma}{(E_b - E_a - \hbar\omega)^2 + \hbar^2\gamma^2/4} \ . \tag{15}$$

We would like to apply Eq. (15) to the problem of absorption in amorphous semiconductors.

In amorphous semiconductors short-range order plays a key role in the absorption process. Locally, the electronic states of the amorphous solid may be considered to be a broadened superposition of molecular-orbital states.[13] For example, in tetrahedrally coordinated covalent materials, linear combinations of atomic orbitals lead to bonding ($\mid \sigma \rangle$) and antibonding ($\mid \sigma^* \rangle$) molecular states which then broaden into valence and conduction bands when the solid is formed. (See Fig. 1.) In the case of chalcogenide semiconductors, there are three molecular orbitals: bonding, nonbonding, and antibonding states which produce three local bands in the solid. This more complicated case will not be considered here.

As seen in Eq. (15), the maximum value for k occurs when $\hbar\omega = E_b - E_a$. In the following we will assume that maximum absorption occurs when $\hbar\omega = E_{\sigma'*} - E_{\sigma'}$, where $E_{\sigma'*}$ and $E_{\sigma'}$ are energies in the conduction and valence bands such that $E_{\sigma'*} = E_{\sigma*}$ and $E_{\sigma'} = E_\sigma$. This is consistent with the fact that the density of states in the conduction and valence bands is a maximum for $E_{\sigma'*}$ and $E_{\sigma'}$. (See Fig. 1.) If $E_b = E_{\sigma'*}$ and $E_a = E_{\sigma'}$, then $\mid b \rangle = \mid \sigma'^* \rangle$ and $\mid a \rangle = \mid \sigma' \rangle$.

In Eq. (15), Θ is proportional to the number of possible transitions from the valence to the conduction band. Assuming a complete lack of momentum conservation, Θ will depend on the number of occupied states in the
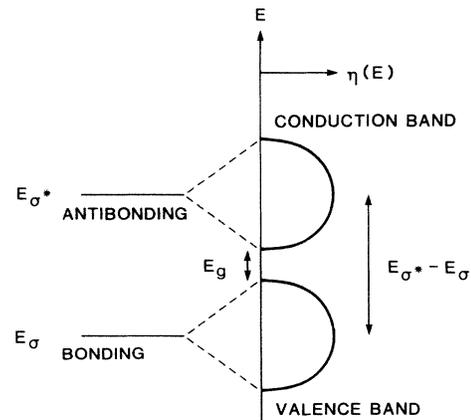

FIG. 1. Molecular-orbital states, $\mid \sigma \rangle$ and $\mid \sigma^* \rangle$ corresponding to energies E_σ and $E_{\sigma*}$, broaden into valence and conduction bands when the solid is formed. $\eta(E)$ represents density of states. E_g represents the energy band gap. When $\hbar\omega = E_{\sigma*} - E_\sigma$ absorption is assumed to be maximum. Adopted from Zallen (Ref. 13).

valence band, $\eta_v(E)f_v(E)dE$, and on the number of unoccupied states in the conduction band, $\eta_c(E')$ $[1-f(E')]dE'$, which are separated by an energy $\hbar\omega$ from states in the valence band.[4] $\eta_v(E)$ and $\eta_c(E)$ represent the density of states in the valence and conduction band, and $f(E)$ represents the Fermi function. Therefore,

$$\Theta \propto \int dE \int dE' \, \eta_v(E)f(E)\eta_c(E')$$
$$\times [1-f(E')]\delta(E'-(E+\hbar\omega)) \qquad (16)$$

or

$$\Theta \propto \int \eta_v(E)f_v(E)\eta_c(E+\hbar\omega)[1-f_c(E+\hbar\omega)]dE \ . \qquad (17)$$

For temperatures which are not too high, semiconductors are insulators, so that $f_v(E)$ is of order unity and $f_c(E+\hbar\omega)$ is of order zero. For this case

$$\Theta \propto \int_{E_{\text{bottom}}-\hbar\omega}^{E_{\text{top}}} \eta_v(E)\eta_c(E+\hbar\omega)dE \ , \qquad (18)$$

where E_{top} represents the energy at the top of the valence band and E_{bottom} represents the energy at the bottom of the conduction band so that the optical energy band gap, E_g, is given by:

$$E_g = E_{\text{bottom}} - E_{\text{top}} \ . \qquad (19)$$

Assuming density of states in the valence and conduction bands can be expressed in terms of energy to some power,[4] i.e.,

$$\eta_v(E) = \text{const} \times (E_{\text{top}} - E)^p \ ,$$

$$\eta_c(E) = \text{const} \times (E - E_{\text{bottom}})^s \ ,$$

Eq. (18) can be evaluated as[4]

$$\Theta = \text{const} \times (\hbar\omega - E_g)^{p+s+1} \ . \qquad (20)$$

If the valence and conduction bands are parabolic so that $p = s = \frac{1}{2}$,

$$\Theta = \text{const} \times (\hbar\omega - E_g)^2 \ . \qquad (21)$$

Assuming this is the case, the extinction coefficient is then determined from (15) and (21) to be

$$k = \text{const} \frac{2\pi}{3} e^2 \hbar^2 |\langle \sigma'^* | \mathbf{x} | \sigma' \rangle|^2$$

$$\times \frac{\gamma}{(E_{\sigma'*} - E_{\sigma'} - \hbar\omega)^2 + \hbar^2\gamma^2/4}(\hbar\omega - E_g)^2 \ . \qquad (22)$$

We can rewrite Eq. (22) in the following form:

$$k(E) = \frac{A(E-E_g)^2}{E^2 - BE + C} \ , \qquad (23)$$

where

$$A = \text{const} \frac{2\pi}{3} e^2 \hbar^2 |\langle \sigma'^* | \mathbf{x} | \sigma' \rangle|^2 \gamma \ , \qquad (24)$$

$$B = 2(E_{\sigma'*} - E_{\sigma'}) \ , \qquad (25)$$

and

$$C = (E_{\sigma'*} - E_{\sigma'})^2 + \hbar^2\gamma^2/4 \ . \qquad (26)$$

It can be seen from Eqs. (24), (25), and (26) that $A > 0$, $B > 0$, $C > 0$, and that $4C - B^2 > 0$. This is important because as we shall show $n(E)$ cannot be determined from Kramers-Kronig analysis unless these conditions are met.

The two seemingly unrelated quantities n and k are related by Kramers-Kronig relations, also known as dispersion relations. These relations are a direct consequence of the analytic behavior of $N(E) = n(E) - ik(E)$. In turn, the analytic behavior of $N(E)$ stems from the principle of causality, which states that no signals can be transmitted through a medium at a speed greater than that of light in vacuum.[10]

A consequence of the analytical behavior of $N(E)$ is that its real and imaginary parts are related by

$$\text{Re}[N(E)] = \frac{1}{\pi} P \int_{-\infty}^{\infty} \frac{\text{Im}[N(E')]}{E'-E} dE' \ , \qquad (27)$$

provided $N(E)$ vanishes at infinity. P denotes Cauchy's principle-value integral.

If $N(E)$ tends to a constant at infinity, Eq. (27) must be replaced by

$$\text{Re}[N(E) - N(\infty)] = \frac{1}{\pi} P \int_{-\infty}^{\infty} \frac{\text{Im}[N(E') - N(\infty)]}{E'-E} dE' \ , \qquad (28)$$

where

$$N(\infty) = \lim_{E\to\infty} N(E) = n(\infty) - ik(\infty) \ .$$

Thus, if the functional form of $k(E)$ is known for all energies then the functional form of $n(E)$ for all energies can be determined.

Assuming Eq. (23) for $k(E)$ holds, $n(E)$ can be found from Eq. (28).

$$n(E) - n(\infty) = \frac{1}{\pi} P \int_{-\infty}^{\infty} \frac{k(E') - k(\infty)}{E'-E} dE' \ . \qquad (29)$$

Or substituting for $k(E)$ given by Eq. (23), we get

$$n(E) - n(\infty) = \frac{1}{\pi} P \int_{-\infty}^{\infty} \frac{A[(B-2E_g)E' + E_g^2 - C]}{(E'^2 - BE' + C)(E' - E)} dE'$$

$$= \frac{1}{\pi}(-2\pi iR - \pi iS) \ , \qquad (30)$$

where R is the residue of the integrand at the pole located in the lower half of the complex E plane, and S is the residue evaluated at the pole located along the real axis [see, e.g., Roman[14] for derivation of the last equality of Eq. (30)].

The pole of the integrand of Eq. (30) in the lower-half plane is at $B/2 - iQ$ where $Q = \frac{1}{2}(4C - B^2)^{1/2}$, and the pole along the real axis is at E. Thus, we obtain

$$n(E) = n(\infty) + \frac{B_0 E + C_0}{E^2 - BE + C} \ , \qquad (31)$$

where

$$B_0 = \frac{A}{Q}\left[-\frac{B^2}{2} + E_g B - E_g^2 + C\right] \qquad (32)$$

and

$$C_0 = \frac{A}{Q}\left[(E_g^2+C)\frac{B}{2}-2E_g C\right] . \tag{33}$$

It is expected that $N(E)-N(\infty)$ is analytic in the lower half of the complex E plane (rather than the upper half of the plane) because $N(E)$ is written as equal to $n(E)-ik(E)$ [rather than $n(E)+ik(E)$]. Indeed, it can be shown that

$$N(E)-N(\infty) \equiv [n(E)-n(\infty)]-i[k(E)-k(\infty)]$$

$$= \frac{A}{Q}\frac{(B-2E_g)(B/2+iQ)+E_g^2-C}{B/2+iQ-E} . \tag{34}$$

which is analytic in the lower half of the complex E plane, since $Q>0$.

It is usually assumed that $n(\infty)$ equals unity.[10] Our results discussed in Sec. III, however, indicate that $n(\infty)>1$ (the exact value depending on the particular material). The above analysis therefore demonstrates that if $k(E)$ is given by Eq. (23), then five parameters, i.e., A, B, C, E_g, and $n(\infty)$, are sufficient to fully describe the dependence of both n and k on E. A method of experimentally determining these parameters from a measured reflectance spectrum will be described in a later paper.[15] Another method of evaluating these parameters from experimentally measured n and k versus E is given in the following section.

III. EXPERIMENTAL VERIFICATION

Energy dependence of both k and n given by Eqs. (23) and (31) can be fully and simultaneously determined if only four of the six parameters E_g, A, B, C, B_0, and C_0 [B_0 and C_0 are not independent parameters according to Eqs. (32) and (33)], together with $n(\infty)$ are specified. In principle, therefore, both n and k as functions of E are simultaneously determined if altogether five values of n and k for specified energies are (experimentally) known, where at least one of which is a value for n. In practice, however, the scheme described below proves to be more useful.

Differentiating $k(E)$ with respect to E and setting dk/dE equal to zero, we find that $k(E)$ has a minimum at

$$E_{min}=E_g , \tag{35}$$

[where, of course, k evaluated at E_g, namely $k(E_g)$, equals zero], and a maximum at E_{max} given by

$$E_{max}=\frac{BE_g-2C}{2E_g-B} . \tag{36}$$

The value of k evaluated at E_{max}, k_{max}, is then

$$k_{max}=\frac{4A(E_g^2-BE_g+C)}{4C-B^2} . \tag{37}$$

Let us also assume that the value of k at an arbitrary point E_{fit} (different from E_g and E_{max}) is known and has a finite value equal to k_{fit}, namely,

$$k_{fit}=\frac{A(E_{fit}-E_g)^2}{E_{fit}^2-BE_{fit}+C} . \tag{38}$$

Simultaneous solution of Eqs. (35)—(38) yields E_g, A, B, and C in terms of E_{min}, E_{max}, k_{max}, and k_{fit}:

$$B=\frac{B_2+(B_2^2-4A_2C_2)^{1/2}}{2A_2} ,$$

where

$$A_2=(E_g-\alpha)(E_{fit}-\alpha)+L ,$$

$$B_2=(E_g-\alpha)(E_{fit}^2-\beta)+(E_{fit}-\alpha)(E_g^2-\beta)+4L\alpha ,$$

and

$$C_2=(E_g^2-\beta)(E_{fit}^2-\beta)+4L\beta ,$$

with

$$\alpha=\frac{E_{max}+E_g}{2} ,$$

$$\beta=E_g E_{max} ,$$

and

$$L=\frac{k_{max}(E_{fit}-E_g)^2}{4k_{fit}} .$$

After B is evaluated, C and A are then given by

$$C=\alpha B-\beta$$

and

$$A=k_{fit}(E_{fit}^2-BE_{fit}+C)/(E_{fit}-E_g)^2 .$$

Therefore, if E_{min}, E_{max}, k_{max}, and k_{fit} (given in Table I for various films) are known, then E_g, A, B, and C are determined, and thus k as a function of E is completely defined.

As discussed in Sec. II, n as a function of E can be determined from $k(E)$ and is given by Eq. (31), where B_0 and C_0 are evaluated through Eqs. (32) and (33). However, in order to specify $n(\infty)$ we must know the value of n at an arbitrary point E'_{fit}, i.e., $n_{fit}=n(E'_{fit})$ must be known. Here, E'_{fit} may or may not be equal to E_{fit}. In this paper, for the most part, E'_{fit} is taken at 1.959 eV, equivalent to a wavelength of 632.8 nm (the He-Ne laser wavelength usually used in ellipsometric measurement of refractive index n).

Values of the given parameters presented in Table I were either taken directly from the cited references, or were deduced from available data.

As seen in Figs. 2—9 and described below, the experimentally determined n and k of various amorphous semiconductor and dielectric thin films indeed obey dispersion relations given by Eqs. (23) and (31).

A. a-Si and a-Si:H

Amorphous silicon (a-Si) and hydrogenated amorphous silicon (a-Si:H) semiconducting thin films are widely used in microelectronic devices,[16] solar-energy cells,[17] optical media,[18-20] and radiation detectors.[21] Their optical and electrical properties have, therefore, been previously studied in detail. The measured optical constants, i.e., n and k, over a wide range of energies, of a variety of a-Si and

A. R. FOROUHI AND I. BLOOMER

TABLE I. Data for $E_{min} = E_g$, E_{max}, k_{max}, k_{fit}, and n_{fit} used to evaluate A, B, C, B_0, C_0, and $n(\infty)$.

Film characterization					Given values measured, observed, or deduced			
Film ID no. in the original reference	Film	Preparation method (ambient)	at. %H	$E_{min} = E_g$ (eV)	E_{max} (eV)	k_{max}	$k_{fit}(E_{fit})^c$	$n_{fit}(E'_{fit})^c$
2	a-Si[a]	Sputtering (Ar/H₂)	not given	1.3	4.33	2.2	0.52(2.3)	4(1.959)
3	a-Si[a]	Glow discharge	not given	1.65	4.55	2.55	0.55(2.5)	4.05(1.959)
1	a-Si	Sputtering (Ar)	0	0.95	3.45	2.5	0.5(1.95)	5(1.959)
3	a-Si:H	Sputtering (Ar/H₂)	8–10	1.15	3.95	2.5	0.5(2.3)	4.3(1.959)
4	a-Si:H	Sputtering (Ar/H₂)	20–30	1.35	4.15	2.5	0.5(2.5)	3.8(1.959)
5	a-Si:H	Glow discharge	20–30	0.475	3.975	1.7	0.3(2.375)	3.3(1.959)
	a-Si	Electron-beam evaporation	0	1.3	4	2.89	1.384(2.6)	4.213(3)
	a-Si₃N₄	Pyrolytic	negligible	4.75	10.5	1.53	0.866(7.75)	2.492(8.5)
	a-TiO₂[b]	Anodic oxidation of titanium	not applicable	2.8	4.768	1.485	0.65(3.875)	3.148(4.133)

[a]Expect the films to be a-Si:H due to their preparation methods.
[b]Noncrystalline titanium oxide, probably with poorly defined stoichiometry.
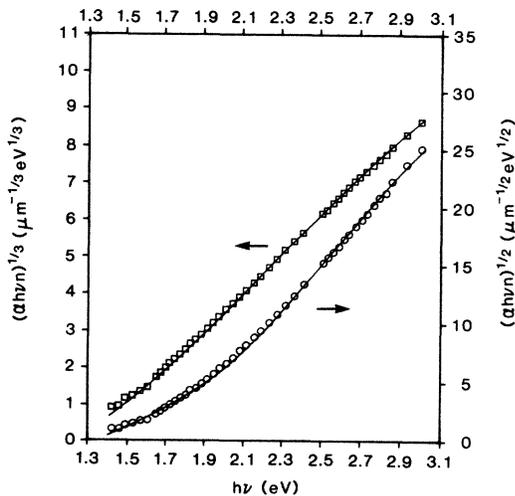[c]The numbers in parenthesis represent E_{fit} and E'_{fit} in eV.

FIG. 2. The solid lines in this figure as well as Figs. 3–9 are theoretical plots. The analytical form of n and k are given by Eqs. (31) and (23) with the constants specified in Table I. The experimental data points are from Klazes et al. (Ref. 2) for a-Si produced by sputtering of crystalline silicon in Ar/H₂ ambient (film number 2). [Solid lines in this figure and Fig. 3 represent plot of $(\alpha h\nu n)^{1/2} = (10.136E^2nk)^{1/2}$ and $(\alpha h\nu n)^{1/3} = (10.136E^2nk)^{1/3}$ versus $h\nu = E$.]

a-Si:H which were prepared by different methods under various process conditions are presented in books and numerous articles.[2-4,22-37] These studies demonstrate that amorphous silicon and hydrogenated amorphous silicon films having different optical properties can be produced if preparation methods are changed. This is in contrast to, e.g., crystalline silicon where a unique set of data[38] does, in principle, describe its optical properties.

(i). Experimental data presented in Figs. 2 and 3 are from Klazes et al.[2] The films were produced by rf reactive sputtering of crystalline silicon in a mixture of argon and hydrogen, and by capacitance rf glow-discharge decomposition of silane (SiH₄) diluted in argon. They were deposited on glass or fused silica substrates at deposition temperatures of 200 °C and 370 °C for sputtering and glow discharge, respectively.

The optical constants were determined by measuring the spectral reflectance and transmittance of the film-substrate system at photon energies between 0.6 and 3.2 eV.

Although the films are presented as a-Si in the original reference, it may be more appropriately presented as a-Si:H, since films prepared by both sputtering in the presence of hydrogen and glow-discharge decomposition of SiH₄ would incorporate hydrogen in the film.

In Figs. 2 and 3, $(\alpha h\nu n)^{1/3}$ and $(\alpha h\nu n)^{1/2}$ are plotted versus $h\nu$, where α denotes absorption coefficient given

OPTICAL DISPERSION RELATIONS FOR AMORPHOUS . . .

TABLE I. (Continued).

Evaluated constants						Original references
A	B	C	B_0	C_0	$n(\infty)$	
1.2331	5.2631	9.1867	0.4005	3.8846	2.2792	Klazes *et al.* (Ref. 2)
1.5690	5.5311	9.6390	0.8298	2.6444	2.4330	
0.9000	5.1000	7.9425	−0.8400	5.5980	2.7908	McKenzie *et al.* (Ref. 3)
0.8494	5.9972	10.7504	−1.0623	7.3507	2.4440	
0.8494	6.3972	11.9898	−1.0623	7.5631	2.1362	
0.2242	7.0266	13.7460	−1.4822	6.8215	2.2739	
1.4910	5.2139	8.6170	0.1242	4.9351	1.5256	Philipp (Ref. 39)
0.8000	14.9868	64.4000	0.2010	11.1000	1.1089	Philipp (Ref. 40)
0.5189	8.1605	17.5291	−0.4195	2.9587	1.7614	Joseph (Ref. 44)

by $\alpha = 4\pi k/\lambda$ and $h\nu$ denotes photon energy E. Klazes *et al.*[2] argued that $(\alpha h\nu n)^{1/3} \sim (h\nu - E_g)$ provides a better fit to their experimental data than $(\alpha h\nu n)^{1/2} \sim (h\nu - E_g)$, from which they deduced optical band gap E_g using a linear extrapolation of $(\alpha h\nu n)^{1/3}$ as a function of photon
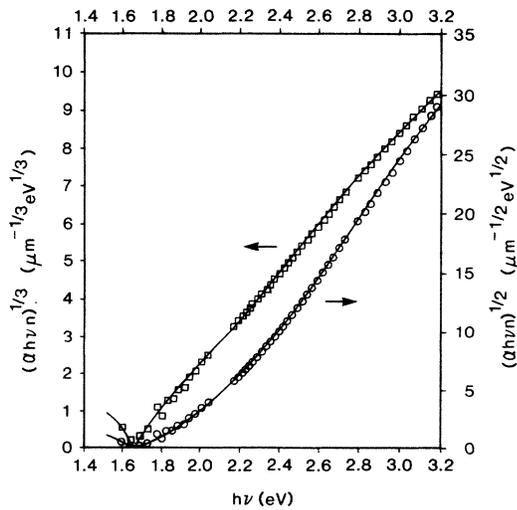
FIG. 3. The experimental data points are from Klazes *et al.* (Ref. 2) for *a*-Si produced by glow-discharge decomposition of SiH₄ (film number 3).

energy $h\nu$. However, as seen in Figs. 2 and 3 a remarkably good fit was found between the experimental data and the corresponding theoretical curves, using formulas (23) and (31). The fit is such that the theoretical curves even pass smoothly through the two "apparently" misplaced data points at $h\nu \cong 1.6$ eV in Fig. 3.

(ii). Experimental data presented in Figs. 4—6 are from McKenzie *et al.*[3] The *a*-Si and *a*-Si:H films were de-
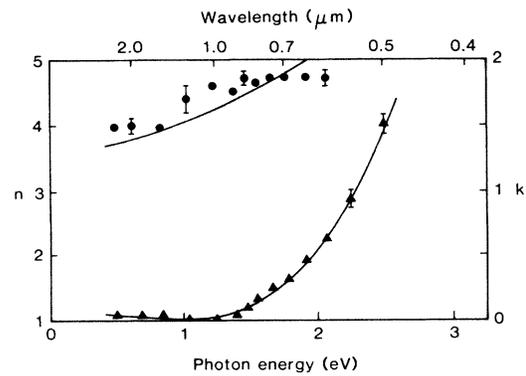

FIG. 4. The experimental data points are from McKenzie *et al.* (Ref. 3). ●, ▲: n and k for *a*-Si produced by sputtering of crystalline silicon in Ar ambient (film number 1).
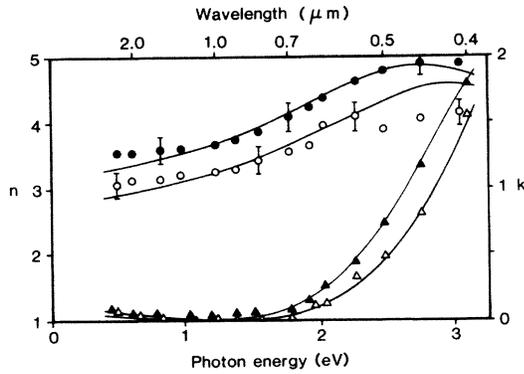
FIG. 5. The experimental data points are from McKenzie et al. (Ref. 3). ●, ▲: n and k for a-Si:H produced by sputtering of crystalline silicon in Ar/H₂ ambient (film number 3). ○, △: n and k for a-Si:H with a different hydrogen content, also produced by sputtering of crystalline silicon in Ar/H₂ ambient (film number 4).

posited on heated (50 °C—200 °C) optical glass substrates, by dc magnetron reactive sputtering of crystalline silicon in an argon-hydrogen plasma, and by dc magnetron glow-discharge decomposition of silane in argon ambient. Values of n and k were determined by measuring spectral reflectance and transmittance of the film-substrate system at photon energies between 0.5 and 3.1 eV.

Evidence for the existence of an energy in the lower end of the spectrum at which k goes through a minimum is clearly seen in Figs. 3—5. The corresponding energy of the minimum of $k(E)$ is E_g in our formulation.

(iii). Experimental data presented in Fig. 7 are from Philipp.[39] The amorphous silicon thin film was formed on unheated glass substrate by electron-beam evaporation of crystalline silicon. The optical constants were determined by Kramers-Kronig analysis of measured reflectance spectra. The poor correspondence between the experimental and theoretical n in Fig. 7, as well as Fig. 8, is probably due to errors introduced by extrapolation of reflectance data to the limits of integrations.[40]
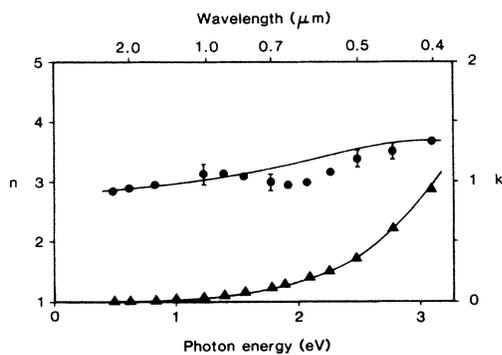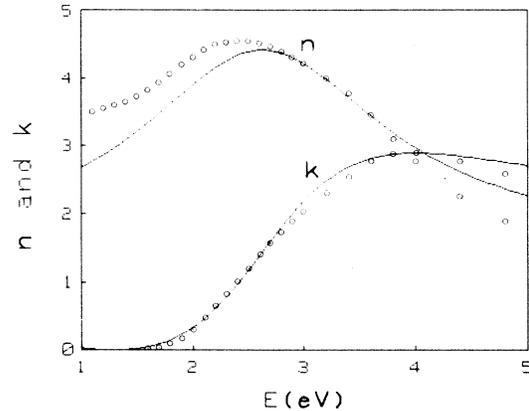

FIG. 7. The experimental data points are from Philipp (Ref. 39) for a-Si produced by electron-beam evaporation.

B. a-Si₃N₄

Dielectric thin films of amorphous silicon nitride (a-Si₃N₄) having different optical properties can also be produced if process conditions are varied.[6,40–43] For example, Forouhi[6] has shown that a minute amount of excess silicon can transform an essentially transparent silicon nitride film into an opaque one in the near-ultraviolet range.

Experimental data presented in Fig. 8 are from Philipp.[40] The noncrystalline silicon nitride film was deposited on bare single crystal silicon or quartz substrate by pyrolytic decomposition at 1000 °C of a mixture of SiH₄ and NH₃. (Silicon nitride prepared by high-temperature pyrolysis is generally considered to be stoichiometric Si₃N₄,[40] containing a negligible amount of hydrogen.) The optical constants were determined by Kramers-Kronig analysis of reflectance and absorption data.

C. a-TiO₂

The optical constants of the semiconducting-dielectric noncrystalline titanium dioxide (a-TiO₂) thin films found

FIG. 6. The experimental data points are from McKenzie et al. (Ref. 3). ●, ▲: n and k for a-Si:H produced by glow-discharge composition of SiH₄ (film number 5).
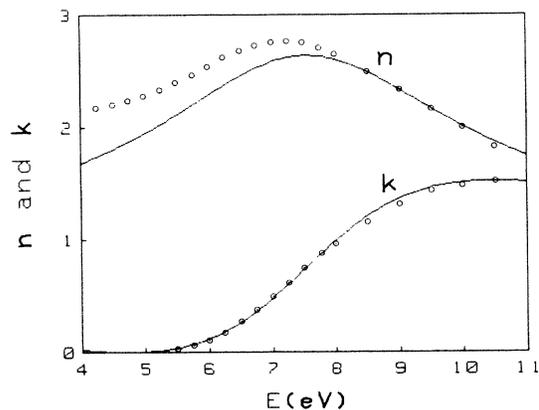

FIG. 8. The experimental data points are from Philipp (Ref. 40) for a-Si₃N₄ produced by pyrolytic decomposition of a mixture of silane and ammonia.
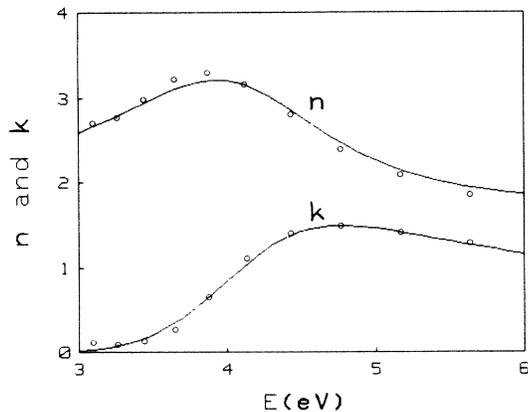
FIG. 9. The experimental data points are from Joseph[44] for a-TiO_2 produced by anodic oxidation of titanium.

in the literature show large differences, probably due to poorly defined composition (in spite of being referred to as TiO_2) caused by differences in preparation methods.

Experimental data presented in Fig. 9 are from Joseph.[44] The film was produced by anodic oxidation of titanium sample. Although not explicitly discussed by

Joseph and Gagnaire,[45] the film is most likely amorphous and not of rutile structure, the crystalline form of natural titanium dioxide. This is because rutile is optically anisotropic, whereas the titanium dioxide investigated by Joseph and Gagnaire[45] appears to be isotropic. The optical constants were determined[45] from analysis of ellipsometric measurements on a set of samples with different film thicknesses, in the wavelength range 220—720 nm, corresponding to 5.6—1.8 eV.

Thus we see that the measured optical constants, n and k, over a wide range of energies, for a variety of a-Si and a-Si:H, a-Si_3N_4, as well as for a-TiO_2, all appear to follow the simple analytical form given by Eqs. (31) and (23).

ACKNOWLEDGMENTS

[1]J. Tauc, R. Grigorovici, and A. Vancu, Phys. Status Solidi 15, 627 (1966).

[2]R. H. Klazes, M. H. L. M. van den Broek, J. Bezemer, and S. Radelaar, Philos. Mag. B 45, 377 (1982).

[3]D. R. McKenzie, N. Savvides, R. C. McPhedran, L. C. Botten, and R. P. Netterfield, J. Phys. C 16, 4933 (1983).

[4]N. F. Mott and E. A. Davis, Electronic Processes in Non-Crystalline Materials, 2nd ed. (Clarendon, Oxford, 1979).

[5]J. Bauer, Phys. Status. Solidi. A 39, 411 (1977).

[6]A. Rahim Forouhi, Electrochem. Soc. Extended Abstract No. 60, 85-1, 82 (1985).

[7]T. S. Moss, G. J. Burrell, and B. Ellis, Semiconductor Opto-Electronics (Wiley, New York, 1973).

[8]T. Bååk, Appl. Opt. 21, 1069 (1982).

[9]G. K. Hubler, C. N. Waddell, W. G. Spitzer, J. E. Fredrickson, S. Prussin, and R. G. Wilson, J. Appl. Phys. 50, 3294 (1979).

[10]See, for example, H. M. Nussenzveig, Causality and Dispersion Relations (Academic, New York, 1972), and references therein.

[11]J. J. Sakurai, Advanced Quantum Mechanics (Addison-Wesley, Reading, Mass., 1967).

[12]W. Heitler, The Quantum Theory of Radiation, 3rd ed. (Dover, New York, 1984).

[13]R. Zallen, The Physics of Amorphous Solids (Wiley, New York, 1983).

[14]P. Roman, Advanced Quantum Theory (Addison-Wesley, Reading, Mass., 1965).

[15]A. R. Forouhi (unpublished).

[16]W. E. Spear, P. G. Le Comber, S. Kinmond, and M. H. Brodsky, Appl. Phys. Lett. 28, 105 (1976).

[17]D. E. Carlson and C. R. Wronski, Appl. Phys. Lett. 28, 671 (1976).

[18]M. A. Bösch, Appl. Phys. Lett. 40, 8 (1982).

[19]M. Janai and F. Moser, J. Appl. Phys. 53, 1385 (1982).

[20]R. D. McLeod, W. Pries, H. C. Card, and K. C. Kao, Appl. Phys. Lett. 45, 628 (1984).

[21]S. N. Kaplan, J. R. Morel, T. A. Mulera, V. Perez-Mendez, G. Schnurmacher, and R. A. Street, IEEE Nucl. Sci. Trans. (to be published).

[22]M. H. Brodsky, R. S. Title, K. Weiser, and G. D. Pettit, Phys. Rev. B 1, 2632 (1970).

[23]H. R. Philipp, J. Phys. Chem. Solids 32, 1935 (1971).

[24]D. T. Pierce and W. E. Spicer, Phys. Rev. B 5, 3017 (1972).

[25]G. A. N. Connell and W. Paul, J. Non-Cryst. Solids 8-10, 215 (1972).

[26]J. Tauc, in Amorphous and Liquid Semiconductors, edited by J. Tauc (Plenum, New York, 1974), p. 159.

[27]E. C. Freeman and W. Paul, Phys. Rev. B 20, 716 (1979).

[28]G. D. Cody, B. Abeles, C. R. Wronski, B. Brooks, and W. A. Lanford, J. Non-Cryst. Solids 35-36, 463 (1980).

[29]S. Al Jalali and G. Weiser, J. Non-Cryst. Solids 41, 1 (1980).

[30]G.-J Jan, F. H. Pollak, and R. Tsu, Sol. Energy Mat. 8, 241 (1982).

[31]J. T. Lue, O. Meyer, J. Lombaard, and R. H. Wang, Solid-State Electron. 25, 1011 (1982).

[32]P. J. Martin, R. P. Netterfield, W. G. Sainty, and D. R. McKenzie, Thin Solid Films 100, 141 (1983).

[33]The Physics of Hydrogenated Amorphous Silicon, edited by J. D. Joannopoulos and G. Lucovsky (Springer-Verlag, New York, 1983), Vols. I and II.

[34]S. P. Coulibaly, J. M. Berger, F. De Chelle, S. Girard, J. P. Ferraton, and A. Donnadieu, J. Non-Cryst. Solids 64, 11 (1984).

[35]F. B. Ellis, Jr., R. G. Gordon, W. Paul, and B. G. Yacobi, J.

Appl. Phys. 55, 4309 (1984).

[36]G. D. Cody, in *Semiconductors and Semimetals,* edited by J. I. Pankove (Academic, New York, 1984), Vol. 21B, p. 11.

[37]H. Piller, in *Handbook of Optical Constants of Solids,* edited by E. D. Palik (Academic, New York, 1985), p. 571.

[38]D. E. Aspnes and A. A. Studna, Phys. Rev. B **27**, 985 (1983).

[39]H. R. Philipp (private communication); also, see Ref. 23.

[40]H. R. Philipp, in *Handbook of Optical Constants of Solids,*

edited by E. D. Palik (Academic, New York, 1985), p. 771.

[41]K. E. Bean, P. S. Gleim, R. L. Yeakley, and W. R. Runyan, J. Electrochem. Soc. **114**, 733 (1967).

[42]H. R. Philipp, J. Electrochem. Soc. **120**, 295 (1973).

[43]M. J. Rand and D. R. Wonsidler, J. Electrochem. Soc. **125**, 99 (1978).

[44]J. Joseph (private communication); also, see Ref. 45.

[45]J. Joseph and A. Gagnaire, Thin Solid Films **103**, 257 (1983).